energies

MDPI

Article

Modeling an Electrolyzer in a Graph-Based Framework

Buu-Van Nguyen *, Johan Romate and Cornelis Vuik

Delft Institute of Applied Mathematcis, Delft University of Technology, Mekelweg 4, 2628CD Delft, The Netherlands; c.vuik@tudelft.nl (C.V.)

* Correspondence: b.nguyen@tudelft.nl

Abstract: We propose a linear electrolyzer model for steady-state load flow analysis of multi-carrier energy networks, where the electrolyzer is capable of producing hydrogen gas and heat. For our electrolyzer model, we show that there are boundary conditions that lead to a well-posed problem. We derive these conditions for two cases, namely with a known and unknown heat efficiency parameter. Furthermore, the derived conditions are validated numerically. Moreover, we investigate the extensibility of our model by including nonlinear models from electricity, gas, and heat. In this setting, we derived boundary conditions based on our previous findings. Due to the involvement of nonlinearity, it is a challenge to prove that the boundary conditions lead to a well-posed problem. Therefore, we simulated the electrolyzer connected with an electricity, gas, and heat system. Additionally, we considered a known and unknown heat efficiency parameter. The numerical results support that the linear electrolyzer model is solvable in a multi-carrier energy network.

Keywords: electrolyzer; integrated energy system; steady-state load flow analysis

1. Introduction

The current level of greenhouse gas emissions leads to a significant contribution towards global warming [1,2]. A straightforward solution to global warming is to reduce the level of emissions. This can be achieved by partly replacing fossil fuels with renewable energy sources, such as solar and wind energy [3,4]. A problem with renewables is that this can lead to an unstable power system [5–7]. This instability is caused by a variable energy production, due to the dependence on the weather. One way to prevent such instabilities is using electrolyzers in the energy system. An electrolyzer can convert a surplus of electricity into hydrogen gas and heat [6,8]. Conversely, when an insufficient amount of energy is produced, the hydrogen gas produced by electrolyzers can be utilized to offset the deficiency. However, utilizing an electrolyzer efficiently requires a careful analysis of the placement and quantity of electrolyzers in the energy network. This analysis is usually achieved by modeling the energy transport, also known as a load flow analysis. Therefore, we are interested in modeling an electrolyzer for load flow analysis, as part of a multi-carrier energy system.

One way to model multi-carrier energy systems is by using a graph-based framework [9–11]. Within this framework, single-carrier energy systems are coupled through conversion units. In this paper, we propose a simplified electrolyzer model that interacts with electricity, gas, and heat for steady-state load flow. The simplified model allows us to analyze well-posedness in an algebraic way. From this analysis, we are able to derive conditions to implement an electrolyzer within this framework. The analysis is performed in a generic way, such that any feasible load profile can be considered.

check for updates

Academic Editor: Shengchun Yang

Received: 16 December 2024
Revised: 22 January 2025
Accepted: 24 January 2025
Published: 5 February 2025

Citation: Nguyen, B.-V.; Romate, J.; Vuik, C. Modeling an Electrolyzer in a Graph-Based Framework. *Energies* **2025**, *18*, 729. https://doi.org/10.3390/en18030729

In the current body of literature, one can find steady-state electrolyzer models that interact with gas and electricity in [12]. To include the interaction with heat, one can model an additional unit, which is an electrical boiler model, as seen in [13]. Whilst this is an alternative to modeling an electrolyzer with two units, it will be more convenient in our analysis to consider modeling it as one unit. In [8], the authors utilized an electrolyzer model that interacts with the three relevant energy carriers. Moreover, they proposed a model that takes into account degradation, which influences the efficiency of the electrolyzer. For long-term planning, this is an important feature, but in steady-state load flow analysis, we can assume a constant value for a given time frame. A different electrolyzer model interacting with all relevant carriers was introduced in [14]. The model takes time into consideration. Other models that include transient effects for real-time simulation can be found in [6,15]. In steady-state load flow analysis, we assume that the transient effects have stabilized. Therefore, we do not require these effects. A factor that plays a role in energy conversion is the time lag. For example, a heat network operates on a different time-scale than an electrical network. E.g., heat takes more time to be transported than electricity. A model that considers this effect is proposed in [16]. This effect is more suitable for market matching purposes and real-time simulations. Table 1 shows an overview of the carriers included in the electrolyzer models.

Table 1. A comparison between relevant works and the method proposed in this paper. Electricity, gas, and heat are the energy carriers included in the model. Time corresponds to a time-based model.

Reference	Purpose	Electricity	Gas	Heat	Time
[12]	Design	✓	✓		
[6]	Operational	✓	✓	-	✓
[15]	Operational	✓	✓	-	✓
[8]	Cost analysis	✓	✓	✓	✓
[14]	Operational	✓	✓	✓	✓
Proposed	Design	✓	✓	✓	-

Our key features in this paper concern the following:

- We introduce a simplified model of an electrolyzer with conversion to gas and heat for steady-state load flow analysis. We simplify the model to its core, which is the conversion of electricity into gas and heat.
- The simplification enables an algebraic approach, to verify if the model is mathematically sound. We achieve this by analyzing well-posedness for different use cases.
- The findings are supported numerically.

The paper is structured as follows. In Section 2, the electrolyzer model is introduced. Section 3 shows that boundary conditions exist that lead to a well-posed problem. Section 4 includes some numerical experiments to illustrate our approach. We conclude with remarks in Section 5.

2. Model

We model an electrolyzer that can convert electricity into gas and residual heat, where we are interested in two cases. The first case considers an electrolyzer that converts gas and heat with a known output ratio. The second case considers a situation where the output ratio has to be determined depending on the energy transport surrounding the electrolyzer.

Before we start with the model equations, we need a graph representation of an electrolyzer. Therefore, we describe how an energy network can be transformed into a

graph. A graph consists of nodes connected by links. Each node and link corresponds to an energy network element. For example, a node can represent a source, and a link can represent a transmission line. Moreover, each node and link corresponds to a physical law. Explicitly, the nodes are associated with conservation laws and the links are associated with the physical model of the underlying network element. Table 2 shows an overview of the conservation laws and common models for each single-carrier. The models for each single-carrier represent the following: the electrical network is an AC three-phase balanced system [10,17], the gas network is a low-pressure system [10,18], and the heat network is a closed-loop system [10]. An analogous analysis can be performed with a DC system or high-pressure gas system.

Table 2. Models for electricity, gas, and heat networks.

	Network Element	Description	Model
Electricity	Node	Kirchhoff's law for active power	$P_i = -\sum_j P_{ij}$
	Node	Kirchhoff's law for reactive power	$Q_i = -\sum_j Q_{ij}$
	Link	Short transmission line (send, P)	$P_{ij} = g_{ij}\lvert V_i\rvert^2 - \lvert V_i\rvert\lvert V_j\rvert\left(g_{ij}\cos\delta_{ij} + b_{ij}\sin\delta_{ij}\right)$
	Link	Transmission line (send, Q)	$Q_{ij} = -b_{ij}\lvert V_i\rvert^2 - \lvert V_i\rvert\lvert V_j\rvert\left(g_{ij}\sin\delta_{ij} - b_{ij}\cos\delta_{ij}\right)$
	Link	Transmission line (receive, P)	$P_{ji} = g_{ij}\lvert V_j\rvert^2 - \lvert V_i\rvert\lvert V_j\rvert\left(g_{ij}\cos\delta_{ij} - b_{ij}\sin\delta_{ij}\right)$
	Link	Transmission line (receive, Q)	$P_{ji} = -b_{ij}\lvert V_j\rvert^2 + \lvert V_i\rvert\lvert V_j\rvert\left(g_{ij}\sin\delta_{ij} + b_{ij}\cos\delta_{ij}\right)$
Gas	Node	Conservation of mass	$q_i = \sum_j q_{ij}$
	Link	Pipe	$p_i - p_j = (C^g)^{-2} f\lvert q_{ij}\rvert q_{ij}$
Heat	Node	Conservation of mass	$m_i = \sum_j m_{ij}$
	Node	Conservation of energy (supply)	$\sum_l m_{i,l} T^s_{i,l} = \sum_j m_{ij} T^s_{ij}$
	Node	Conservation of energy (return)	$\sum_l m_{i,l} T^r_{i,l} = \sum_j m_{ij} T^r_{ij}$
	Link	Pipe	$p_i - p_j = (C^h)^{-2} f\lvert m_{ij}\rvert m_{ij}$
	Link	Pipe heat loss (supply)	$T^s_{ji} = T^a + e^{=\frac{h\pi DL}{C_p m}}\left(T^s_{ij} - T^a\right)$
	Link	Pipe heat loss (return)	$T^r_{ij} = T^a + e^{=\frac{h\pi DL}{C_p m}}\left(T^r_{ji} - T^a\right)$
	Terminal link	Total heat power	$\Delta\varphi_{i,l} = C_p m_{i,l}(T^s_{i,l} - T^r_{i,l})$

Since an electrolyzer interacts with different energy-carriers, it is modeled as a node connected with links of the relevant energy carriers. We assume that these links have no energy losses. The coupling node, that represents an electrolyzer, has a model that governs the energy balance, given by Equation (1):

$$\eta P = \mathrm{HHV} q + \Delta\varphi, \tag{1}$$

where $\eta \in [0, 1]$ is the efficiency, P is the active power, q is the gas flow, HHV is the higher heating value of gas, and $\Delta\varphi$ is the heat power (Appendix A). This model is based on the combined heat and power (CHP) model from [19,20], where we have adjusted our model based on the input and output energy. However, a CHP can generate electricity and heat in a flexible manner, whilst for an electrolyzer, only residual heat is available. This behavior is reflected by Equation (2):

$$\eta_h \eta P = \Delta\varphi, \tag{2}$$

where $\eta_h \in [0, 1]$ is the heat efficiency. In other words, Equation (2) tells us that a fraction of the available energy is converted to heat. Henceforth, we require two equations to model an electrolyzer that converts electricity into gas and heat.

Our model allows the electrolyzer to produce gas and heat in a flexible manner by letting η_h be unknown. Hence, our model is capable of modeling both cases we mentioned

at the beginning of this section. From a mathematical point of view, we seek to know when the model is well-posed for these cases. Hence, in Section 3, we show the necessary conditions for when this holds.

3. Boundary Conditions

In general, integrated energy networks lead to a system of nonlinear equations. These systems are usually solved numerically. Solving a nonlinear energy system is conventionally carried out with the Newton–Raphson (NR) method. In this method, a linearization of the system of equations is involved, where one has to solve a linear system in order to solve the original system. With regards to linear systems, a necessary condition for well-posedness is that the system of equations is square. Usually, energy network models have more variables than equations, unless we allow additional conditions in the form of specifying variables. In this paper, we denote these as boundary conditions. In literature related to electrical networks, nodes with different types of boundary conditions are known as node types, e.g., PQ, PV, and slack nodes.

To understand which conditions need to be met for a well-posed system including an electrolyzer, we start with a simple network. We investigate an electrolyzer with one node of each single-carrier attached to it. The graph representation is shown in Figure 1.

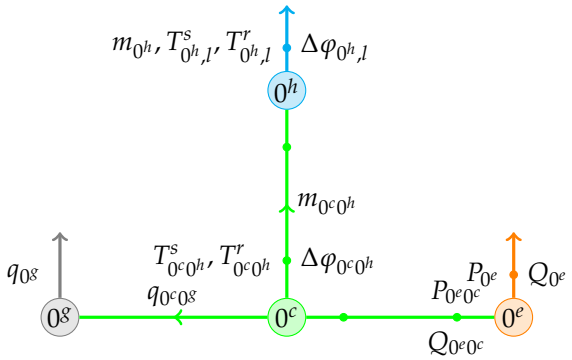

Figure 1. A graph representation of an electrolyzer. Node 0^c and the connecting dummy links represent the electrolyzer. Node 0^g is a node of the gas network. Node 0^h is a node of the heat network. Node 0^e is a node of the electrical network. For each node, except node 0^c, a terminal link is connected to it. This link represents energy flowing in or out of the network.

Well-posedness conditions must hold for elementary cases, such as an electrolyzer only generating one of the energy outputs, gas or heat. This reduces down to a Power-to-Gas (P2G) unit or an electrical boiler. Leading to an analysis of two networks, which are shown in Figures 2 and 3.

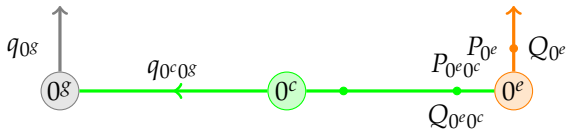

Figure 2. A coupling between an electrical and a gas network with an electrolyzer. This is equivalent to modeling a P2G unit.

Based on our initial model, we can model a P2G unit or an electrical boiler by setting the heat efficiency to 0 or 1. Alternatively, the mass flow $m_{0^c0^h}$ or the gas flow $q_{0^e0^g}$ is set to 0.

In the remainder of this section, we derive boundary conditions for two cases, a known heat efficiency and a unknown heat efficiency.

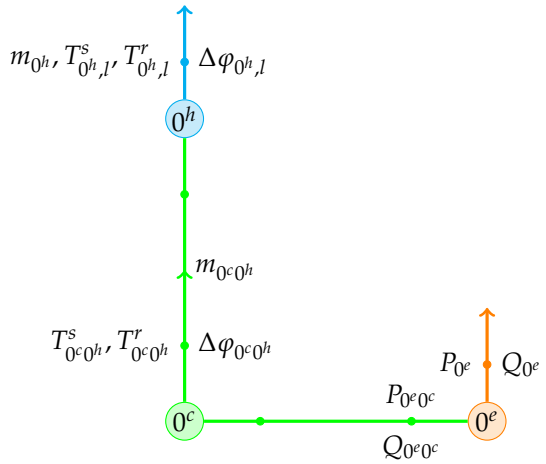

Figure 3. A coupling between an electrical and a heat network with an electrolyzer. This is equivalent to modeling an electrical boiler

3.1. Known Heat Efficiency

In this section, we assume that the heat efficiency η_h of the electrolyzer is given. Furthermore, we are interested in the production of gas and heat based on a given active power. It is also possible to specify the gas flow or heat power instead of the active power, which gives us a similar analysis. Henceforth, we focus on one case, which is the case with a specified active power. We start by deriving the boundary conditions for the P2G unit, then the electrical boiler. Finally, we combine the boundary conditions, leading to well-posedness conditions for the electrolyzer.

3.1.1. P2G

A P2G unit has the following model [21,22]:

$$\eta P = \mathrm{HHV} q, \tag{3}$$

where $\eta \in [0, 1]$. One can obtain an equivalent model with the electrolyzer model (1) and (2) by assuming that $\eta_h = 0$. The system of equations corresponding to the network shown in Figure 2 is represented as

$$P_{0^e} + P_{0^e0^c} = 0 \tag{4}$$
$$Q_{0^e} + Q_{0^e0^c} = 0 \tag{5}$$
$$q_{0^c0^g} - q_{0^g} = 0 \tag{6}$$
$$\eta P_{0^e0^c} - \mathrm{HHV} q_{0^c0^g} = 0. \tag{7}$$

We require a square system for well-posedness. HHV is a known parameter, so we have four equations and six unknown variables. To obtain a square system we must specify two variables.

We assume that the input energy, P_{0^e}, is known. We let $Q_{0^e,0^c} = 0$. This choice is motivated from a physical point of view. Note that we have an AC model for the electrical network. The electrolyzer model (3) does not depend on the reactive power, because we assume that an electrolyzer requires a DC input [6]. We also assume that there are no energy losses from converting AC to DC. Hence, the reactive power can be any arbitrary constant. We have chosen 0 for convenience. With these assumptions, we now have a square system and the boundary conditions are presented in Table 3.

Table 3. Known heat efficiency: boundary conditions for a P2G unit.

Node	Known	Unknown
0^g		q_{0^g}
0^e	P_{0^e}	Q_{0^e}
0^c	$Q_{0^e0^c} = 0$	$q_{0^c0^g}, P_{0^c0^e}$

Note that the system is linear. The chosen boundary conditions lead to a non-singular matrix. Therefore, a unique solution exists. Thus, our boundary conditions lead to a well-posed problem.

3.1.2. Electrical Boiler

An electrical boiler is modeled with [23]:

$$\Delta\varphi_{0^c0^h} = \eta P_{0^e0^c}, \tag{8}$$

This model is equivalent to the electrolyzer model (1) and (2) whenever $\eta_h = 1$, because this results in $q_{0^c0^h} = 0$. We consider the model described in Equation (8) for the sake of brevity. The network shown in Figure 3 results in the following system of equations:

$$P_{0^e} + P_{0^e0^c} = 0 \tag{9}$$
$$Q_{0^e} + Q_{0^e0^c} = 0 \tag{10}$$
$$m_{0^c0^h} - m_{0^h} = 0 \tag{11}$$
$$m_{0^c0^h} T^s_{0^c0^h} - m_{0^h} T^s_{0^h,l} = 0 \tag{12}$$
$$-m_{0^c0^h} T^r_{0^c0^h} + m_{0^h} T^r_{0^h,l} = 0 \tag{13}$$
$$C_p m_{0^h}(T^s_{0^h,l} - T^r_{0^h,l}) - \Delta\varphi_{0^h,l} = 0 \tag{14}$$
$$\eta P_{0^e0^c} - \Delta\varphi_{0^c0^h} = 0 \tag{15}$$
$$C_p m_{0^c0^h}(T^s_{0^c0^h} - T^r_{0^c0^h}) - \Delta\varphi_{0^c0^h} = 0. \tag{16}$$

Equation (16) is a new addition compared to the P2G case. This equation is required, because it describes how the heat consumption is related to the mass flow and temperature for a heat sink and source.

We assume that the specified heat constant C_p is known. It follows that our system has eight equations and 12 unknowns. To obtain a square system, we have to specify four variables. We let the electrolyzer generate heat with a specified active power P_{0^e}. Resulting in node 0^e being a load node. From Equations (14) and (16), it follows that a reference temperature is required for a unique solution. Thus, we assume that the return temperature $T^r_{0^h,l}$ is specified. The third variable to be specified is the supply temperature of the electrical boiler $T^s_{0^c0^h}$, because we assume that the provided heat comes out at a set temperature. The last variable we specify is the reactive power, $Q_{0^e0^c} = 0$. This choice is made with the same reasoning as for the P2G unit. The assumptions are summarized in Table 4.

Table 4. Known heat efficiency: boundary conditions for an electrical boiler.

Node	Known	Unknown
0^h	$T^r_{0^h,l}$	$m_{0^h}, T^s_{0^h,l}, \Delta\varphi_{0^h,l}$
0^e	P_{0^e}	Q_{0^e}
0^c	$Q_{0^c0^e} = 0, T^s_{0^c0^h}$	$m_{0^c0^h}, T^r_{0^c0^h}, \Delta\varphi_{0^c0^h}, P_{0^c0^e}$

These boundary conditions lead to a unique solution. The derivation is shown below.

1. The reactive power Q_{0^e} is obtained from Equation (10):
$$Q_{0^e} = -Q_{0^e0^c}.$$
2. From Equation (9) we obtain the active power P_{0^e}:
$$P_{0^e} = -P_{0^e0^c}.$$
3. Equation (15) yields the heat power $\Delta\varphi_{0^c0^h}$:
$$\Delta\varphi_{0^c0^h} = \eta P_{0^e0^c}.$$
4. The supply temperature $T^s_{0^h,1}$ is obtained from Equation (12):
$$T^s_{0^h,1} = \frac{m_{0^c0^h}}{m_{0^h}} T^s_{0^c0^h} \overset{(11)}{=} T^s_{0^c0^h}.$$
5. From Equation (13), we express the return temperature $T^r_{0^c0^h}$ as:
$$T^r_{0^c0^h} = \frac{m_{0^h}}{m_{0^c0^h}} T^r_{0^h,1} \overset{(11)}{=} T^r_{0^h,1}.$$
6. Applying the results provided in steps 4 and 5 of Equations (14) and (16) yields the total heat power $\Delta\varphi_{0^c0^h}$:
$$\Delta\varphi_{0^c0^h} = \Delta\varphi_{0^h,1}.$$
7. The mass flow $m_{0^c0^h}$ is obtained from Equation (16):
$$m_{0^c0^h} = \frac{\Delta\varphi_{0^c0^h}}{C_p(T^s_{0^c0^h} - T^r_{0^c0^h})}.$$
8. The mass flow m_{0^h} is derived from Equation (11):
$$m_{0^h} = m_{0^c0^h}.$$

Thus, all variables can be uniquely determined. Henceforth, we can conclude that the conditions shown in Table 4 lead to a well-posed problem.

3.1.3. Electrolyzer

We have derived boundary conditions for the P2G unit and electrical boiler, which can be seen as special cases of the electrolyzer with one output energy. Now we consider the electrolyzer with both its output capabilities. The system of equations is given below:

$$P_{0^e} + P_{0^e0^c} = 0 \tag{17}$$
$$Q_{0^e} + Q_{0^e0^c} = 0 \tag{18}$$
$$q_{0^c0^g} - q_{0^g} = 0 \tag{19}$$
$$m_{0^c0^h} - m_{0^h} = 0 \tag{20}$$

$$m_{0^c0^h} T^s_{0^c0^h} - m_{0^h} T^s_{0^h,l} = 0 \tag{21}$$

$$-m_{0^c0^h} T^r_{0^c0^h} + m_{0^h} T^r_{0^h,l} = 0 \tag{22}$$

$$C_p m_{0^h} (T^s_{0^h,l} - T^r_{0^h,l}) - \Delta\varphi_{0^h,l} = 0 \tag{23}$$

$$C_p m_{0^c0^h} (T^s_{0^c0^h} - T^r_{0^c0^h}) - \Delta\varphi_{0^c0^h} = 0 \tag{24}$$

$$\eta P_{0^e0^c} - \mathrm{HHV} q_{0^c0^g} - \Delta\varphi_{0^c0^h} = 0 \tag{25}$$

$$\eta_h \eta P_{0^e0^c} - \Delta\varphi_{0^c0^h} = 0. \tag{26}$$

Recall that η_h is known. This leads to a system with 10 equations and 14 unknowns. Therefore, we have to specify four variables. We combine the boundary conditions derived for the P2G unit and electrical boiler to obtain boundary conditions for the electrolyzer. This results in the conditions shown in Table 5.

Table 5. Known heat efficiency: boundary conditions for an electrolyzer.

Node	Known	Unknown
0^e	P_{0^e}	Q_{0^e}
0^g		q_{0^g}
0^h	$T^r_{0^h,l}$	$m_{0^h}, T^s_{0^h,l}, \Delta\varphi_{0^h,l}$
0^c	$Q_{0^e0^c} = 0, T^s_{0^c0^h}$	$q_{0^c0^g}, P_{0^c0^e}, m_{0^c0^h}, T^r_{0^c0^h}, \Delta\varphi_{0^c0^h}$

A unique solution can be obtained in a similar fashion as for the electrical boiler. We conclude that the boundary conditions lead to a well-posed problem.

3.2. Unknown Heat Efficiency

Our model allows the electrolyzer to output gas and heat with any arbitrary ratio, which is equivalent to an unknown heat efficiency η_h. Compared to the case with a known heat efficiency, we have to specify an additional variable. Otherwise, there are an infinite amount of choices for the output ratio of gas and heat. We model a case where both output energies are known, so that we have to compute the required input energy for the electrolyzer. This leads to the active power being unknown and the gas flow and heat power being known. We note that other cases with two specified energy streams can be chosen, but these lead to a similar analysis.

We have the same set of equations as in the case with a known heat efficiency. With an unknown heat efficiency, the system has 10 equations and 15 unknowns, so five variables have to be specified. Since we want the output energies to be known, we let node 0^g be a load node and node 0^h be a sink. Hence, we specify q_{0^g} and $\Delta\varphi_{0^h,l}$. The reactive power $Q_{0^e0^c}$, the coupling supply temperature $T^s_{0^c0^h}$, and the return temperature $T^r_{0^h,l}$ are known. These variables follow the same reasoning as for the case with a known heat efficiency. The boundary conditions are shown in Table 6.

Table 6. Unknown heat efficiency: boundary conditions for an electrolyzer.

Node	Known	Unknown
0^g	q_{0^g}	
0^h	$\Delta\varphi_{0^h,l} > 0, T^r_{0^h,l}$	$m_{0^h}, T^s_{0^h,l}$
0^e	P_{0^e}, Q_{0^e}	
0^c	$Q_{0^e0^c} = 0, T^s_{0^c0^h}$	$q_{0^c0^g}, P_{0^c0^e}, m_{0^c0^h}, T^r_{0^c0^h}, \Delta\varphi_{0^c0^h}$

Applying these boundary conditions for our system of equations and solving it in a similar fashion as we have seen in Section 3.1 for the electrical boiler, we obtain a unique solution. Thus, the boundary conditions result in a well-posed problem.

3.3. Electrolyzer Coupled with Single-Carrier Systems

In the previous sections, we investigated a network with one electrolyzer without any physical links connected to it, so energy losses from the connected single-carrier networks were not modeled. To show the effect of an electrolyzer in a more realistic energy network setting, we simply extend the network shown in Figure 1 with one physical link for each single-carrier network. The extended link of the gas and heat network represents a pipe. The link for the electrical network represents a transmission line. The network is shown in Figure 4. To add some context, this network can be seen as a simplified rendition of an electrolyzer connecting an off-shore wind farm with an on-shore gas and heat network.

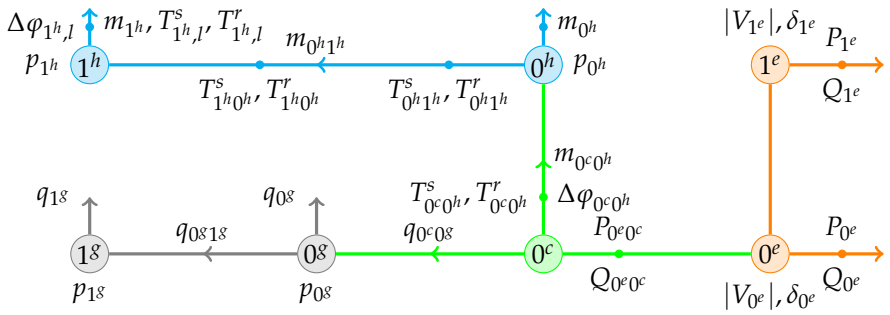

Figure 4. The network shown in Figure 1 is extended with physical links for each energy carrier. Nodes 0^e, 0^g and 0^h act as junctions. Whilst nodes 1^e, 1^g, and 1^h are sources or sinks.

Nodes 0^e, 0^g, and 0^h are junctions. The junctions are modeled in a conventional way by assuming that no energy can enter or escape the network. This forces the load nodes from our previous network (0^e, 0^g, and 0^h) to move to nodes 1^e, 1^g, and 1^h in the current network. The resulting system of equations is shown in Appendix B, which has 18 equations and 30 unknown variables whenever the heat efficiency is known.

For these systems, the same well-posedness conditions derived in Section 3.1 with a known heat efficiency and Section 3.2 with an unknown heat efficiency are applied for loads 1^e, 1^g, and 1^h, because the junctions have basically moved the load nodes. The gas and heat network require reference pressures. The reference pressure can be placed on a junction or a load node in their respective networks. We have chosen to place them on the loads. In addition, the coupling node 0^c has the same boundary conditions that we derived before. The resulting boundary conditions that lead to well-posedness for a known and unknown heat efficiency are shown in Tables 7 and 8.

Table 7. Known heat efficiency: boundary conditions for an electrolyzer with physical links.

Node	Known	Unknown
0^e	$P_{0^e} = 0, Q_{0^e} = 0$	V_{0^e}, δ_{0^e}
1^e	$P_{1^e}, V_{1^e}, \delta_{1^e}$	Q_{1^e}
0^g	$q_{0^g} = 0$	p_{0^g}
1^g	p_{1^g}	q_{1^g}
0^h	$m_{0^h} = 0$	p_{0^h}
1^h	$p_{1^h}, T^r_{1^h,l}$	$p_{1^h}, T^s_{1^h,l'}, \Delta\varphi_{1^h,l}$
0^c	$Q_{0^e0^c} = 0, T^s_{0^c0^h}$	$q_{0^c0^g}, P_{0^e0^c}, m_{0^c0^h}, T^r_{0^c0^h}, \Delta\varphi_{0^c0^h}$

Table 8. Unknown heat efficiency: boundary conditions for an electrolyzer with physical links.

Node	Known	Unknown
0^e	$P_{0^e} = 0, Q_{0^e} = 0$	V_{0^e}, δ_{0^e}
1^e	V_{1^e}, δ_{1^e}	P_{1^e}, Q_{1^e}
0^g	$q_{0^g} = 0$	p_{0^g}
1^g	$q_{1^g} > 0, p_{1^g}$	
0^h	$m_{0^h} = 0$	p_{0^h}
1^h	$p_{1^h}, \Delta\varphi_{1^h,l} > 0, T^r_{1^h,l}$	$m_{1^h}, T^s_{1^h,l}$
0^c	$Q_{0^e0^c} = 0, T^s_{0^c0^h}$	$q_{0^c0^g}, P_{0^e0^c}, m_{0^c0^h}, T^r_{0^c0^h}, \Delta\varphi_{0^c0^h}$

An analytical solution is not easy to derive, due to the nonlinear equations in our system. Therefore, we validate our results numerically.

4. Numerical Results

In this section, we numerically solve the system representing an electrolyzer with physical links shown in Figure 4. We do this with a known and unknown heat efficiency. Recall that there are certain assumptions that hold for this energy network. Firstly, the electrical network is modeled as an AC system. Secondly, we assume a low-pressure system for the gas network. Lastly, the heat network is modeled as a closed-loop system with a supply and return line. Specification of the transmission lines, gas, and pipes are summarized in Appendix C. Additionally, the efficiency parameters of the electrolyzer are specified in the same section.

The system of equations has 18 equations and variables. By substitution, we are able to reduce the system to 15 equations and variables. We solve the system with the Newton–Raphson (NR) method, where the stopping criterion is defined as

$$\|F\|_2 \leq 10^{-6}$$

For the inner solve, we use an LU factorization from the SuperLU package version 6.0.1 [24].

The initial guess for the NR method is given in Table 9. Our choices are motivated as follows. The mass flows are chosen such that they are nonzero, otherwise the Jacobian is singular. The supply and return temperatures are determined such that the average of these temperatures equals the temperature of the boundary condition for the supply temperature $T^s_{0^c0^h}$. The pressure in the gas network p_{0^g} is chosen such that the pressure drop is nonzero, because a pressure drop of zero leads to a singular Jacobian, likewise for the pressure p_{0^h} in the heat network. The voltage magnitude $|V_{0^e}|$ is based on a flat start with the same value as the boundary condition. The other variables are set to 0 out of convenience.

With this initial guess, the NR method converges in five iterations. The numerical solution is shown in Table 10.

We observe reasonable energy losses caused by the physical links. In the electrical network, the transmission line shows a loss in active power. In absolute value, it drops by 0.066 MW. For the gas network, we observe a small pressure drop of $\Delta p = 0.003$ bar. Similarly, for the heat network, a pressure drop of $\Delta p = 0.048$ bar is noted. For the supply temperature from node 0^h to 1^h, the temperature drops by 0.27 K. The return temperature in the direction from node 1^h to 0^h drops by 0.208 K. Thus, our model behaves as expected.

Table 9. Known heat efficiency: the initial guess.

Electricity		**Gas**		
$\lvert V_{0^e} \rvert$	δ_{0^e}	p_{0^g}	$q_{0^g 1^g}$	
$\frac{690}{\sqrt{3}}$ V	0 rad	1.05 bar	0 $\frac{\text{kg}}{\text{s}}$	
Heat				
$T^s_{0^h 1^h}$	$T^r_{1^h 0^h}$	p_{0^h}	$T^s_{1^h,l}$	$m_{0^h 1^h}$
353.15 K	313.15 K	6.3 bar	353.15 K	1 $\frac{\text{kg}}{\text{s}}$
Coupling				
$P_{0^e 0^c}$	$q_{0^c 0^h}$	$m_{0^c 0^h}$	$T^r_{0^c 0^h}$	$\Delta\varphi_{0^c 0^h}$
0 MW	0 $\frac{\text{kg}}{\text{s}}$	1 $\frac{\text{kg}}{\text{s}}$	313.15 K	0 MW

Table 10. Known heat efficiency: solution of an electrolyzer with physical links. The values of the boundary conditions are in bold.

Electricity				
$\lvert V_{0^e} \rvert$ 375 V	δ_{0^e} −0.259 rad	$\mathbf{P_{0^e}}$ **0 MW**	$\mathbf{Q_{0^e}}$ **0 MW**	$\lvert \mathbf{V_{1^e}} \rvert$ **398 V**
$\delta_{\mathbf{1^e}}$ **0 rad**	$\mathbf{P_{1^e}}$ **−2.5 MW**	Q_{1^e} −0.662 MW	$P_{0^e 1^e}$ −2.434 MW	$Q_{0^e 1^e}$ 0 MW
$P_{1^e 0^e}$ 2.5 MW	$Q_{1^e 0^e}$ 0.662 MW			
Gas				
p_{0^g} 1.003 bar	$\mathbf{q_{0^g}}$ **0** $\frac{\text{kg}}{\text{s}}$	$\mathbf{p_{1^g}}$ **1 bar**	q_{1^g} 0.013 $\frac{\text{kg}}{\text{s}}$	$q_{0^g 1^g}$ 0.013 $\frac{\text{kg}}{\text{s}}$
Heat				
p_{0^h} 6.048 bar	$\mathbf{m_{0^h}}$ **0** $\frac{\text{kg}}{\text{s}}$	$T^s_{0^h 1^h}(T^s_{0^h})$ 338.15 K	$\mathbf{p_{1^h}}$ **6 bar**	m_{1^h} 5.74 $\frac{\text{kg}}{\text{s}}$
$T^s_{1^h,l}(T^s_{1^h})$ 337.88 K	$\mathbf{T^r_{1^h,l}}$ **323.15 K**	$T^r_{1^h 0^h}(T^r_{1^h})$ 323.15 K	$\Delta\varphi_{1^h}$ 0.354 MW	$m_{0^h 1^h}$ 5.74 $\frac{\text{kg}}{\text{s}}$
Coupling				
$P_{0^e 0^c}$ 2.434 MW	$\mathbf{Q_{0^e 0^c}}$ **0 MW**	$q_{0^c 0^h}$ 0.013 $\frac{\text{kg}}{\text{s}}$	$m_{0^c 0^h}$ 5.74 $\frac{\text{kg}}{\text{s}}$	$\Delta\varphi_{0^c 0^h}$ 0.365 MW
$\mathbf{T^s_{0^c 0^h}}$ **338.15 K**	$T^r_{0^c 0^h}(T^r_{0^h})$ 322.942 K			

For the case with an unknown heat efficiency, we have chosen boundary condition values, such that we have the same numerical solution as for the known heat efficiency case. Compared to the known case, we observe a similar convergence behavior with the NR method.

With the given boundary conditions, the results for the electrolyzer with physical links support the idea that the problem is well-posed. Hence, we have shown numerically that the electrolyzer can be solved in a multi-carrier energy network.

5. Conclusions

We introduced a linear model for an electrolyzer. This model was used for the steady-state load flow analysis of multi-carrier energy networks. Furthermore, we focused on energy networks that consist of three different energy carriers, electricity, gas, and heat. In this context, we were interested in when the inclusion of the electrolyzer model led to a well-posed problem. For the linear model, see Equations (1) and (2), we derived conditions that led to well-posedness and showed that this held analytically by solving the linear system of equations. We extended our analysis to a system with an electrolyzer connected with an electrical, gas, and heat network. The connected networks introduced nonlinear models, which resulted in a nonlinear system of equations. We derived boundary conditions based on the conditions found for the linear case. Since, we have a nonlinear system of equations, proving that it leads to a well-posed problem is a challenge. Hence, we validated the conditions by simulating the aforementioned network with a known and unknown heat efficiency. For both cases, we solved the nonlinear system with the Newton–Raphson method and obtained consistent solutions. Our numerical results support the idea that the problem is well-posed.

The results of the electrolyzer connected with physical links suggest that the links can be replaced with networks, since the boundary conditions connected with the electrolyzer are the determining factor for well-posedness. In other words, if these boundary conditions are chosen such that they coincide with a known or unknown heat efficiency case, then well-posedness is expected for a broader set of network topologies. Therefore, our electrolyzer model can be used in a broader setting than just one physical link per energy carrier.

We have showcased that one can couple different energy carriers in a simple way that is mathematically sound. However, further investigation is needed to evaluate the model's performance when applied to real-world data from operating energy systems.

Author Contributions: Conceptualization, B.-V.N.; Methodology, B.-V.N.; Software, B.-V.N.; Writing—Original Draft, B.-V.N.; Writing—review and editing, J.R. and C.V.; Supervision, J.R. and C.V.; funding acquisition, C.V. All authors have read and agreed to the published version of the manuscript.

Funding: This work is part of the Energy Intranets (NEAT: ESI-BiDa 647.003.002) project, which is funded by the Dutch Research Council NWO, Netherlands in the framework of the Energy Systems Integration & Big Data programme.

Data Availability Statement: Data are available upon request.

Conflicts of Interest: The authors declare that they have no known competing financial interests or personal relationships that could have appeared to influence the work reported in this paper.

Abbreviations

The following abbreviations are used in this manuscript:

AC	Alternating current
CHP	Combined heat and power
DC	Direct current
HHV	Higher heating value
NR	Newton–Raphson
P2G	Power-to-Gas

Appendix A

Table A1. A list of symbols and definitions.

Electricity	
δ	Voltage angle [rad]
P	Active power [W]
Q	Reactive power [var]
V	Voltage phasor [V]
$\|V\|$	Voltage amplitude [V]
Gas	
f	Friction factor
q	Gas flow rate [$\mathrm{kg \cdot s^{-1}}$]
C_g	Pipe constant [$\mathrm{kg^2 \cdot m^2}$]
Heat	
φ	Heat power [W]
$\Delta\varphi$	Total heat power[W]
T	Temperature [K]
m	Mass flow rate [$\mathrm{kg \cdot s^{-1}}$]
C_h	Pipe constant [$\mathrm{kg \cdot m}$]
C_p	Specific heat [$\mathrm{m^2 \cdot K^{-1} \cdot s^{-2}}$]
General	
p	Pressure [Pa]

Appendix B

The system of equations is shown below:

$$P_{0^e} + P_{0^e1^e} + P_{0^e0^c} = 0 \tag{A1}$$

$$Q_{0^e} + Q_{0^e1^e} + Q_{0^e0^c} = 0 \tag{A2}$$

$$P_{1^e} + P_{1^e0^e} = 0 \tag{A3}$$

$$Q_{1^e} + Q_{1^e0^e} = 0 \tag{A4}$$

$$q_{0^c0^g} - q_{0^g1^g} - q_{0^g} = 0 \tag{A5}$$

$$q_{0^g1^g} - q_{1^g} = 0 \tag{A6}$$

$$p_{0^g} - p_{1^g} - (C^g)^{-2} f^g |q_{0^g1^g}| q_{0^g1^g} = 0 \tag{A7}$$

$$m_{0^h1^h} - m_{1^h} = 0 \tag{A8}$$

$$m_{0^c0^h} - m_{0^h1^h} - m_{0^h} = 0 \tag{A9}$$

$$p_{0^h} - p_{1^h} - \left(C^h\right)^{-2} f^h |m_{0^h1^h}| m_{0^h1^h} = 0 \tag{A10}$$

$$m_{0^c0^h} T^s_{0^c0^h} - m_{0^h1^h} T^s_{0^h1^h} = 0 \tag{A11}$$

$$-m_{0^c0^h} T^r_{0^c0^h} + m_{0^h1^h} T^r_{0^h1^h} = 0 \tag{A12}$$

$$m_{0^h1^h} T^s_{1^h0^h} - m_{1^h} T^s_{1^h,l} = 0 \tag{A13}$$

$$-m_{0^h1^h} T^r_{1^h0^h} + m_{1^h} T^r_{1^h,l} = 0 \tag{A14}$$

$$C_p m_{1^h} (T^s_{1^h,l} - T^r_{1^h,l}) - \Delta\varphi_{1^h,l} = 0 \tag{A15}$$

$$C_p m_{0^c0^h} (T^s_{0^c0^h} - T^r_{0^c0^h}) - \Delta\varphi_{0^c0^h} = 0 \tag{A16}$$

$$\eta P_{0^e0^c} - \mathrm{HHV} q_{0^c0^g} - \Delta\varphi_{0^c0^h} = 0 \tag{A17}$$

$$\eta_h \eta P_{0^e0^c} - \Delta\varphi_{0^c0^h} = 0 \tag{A18}$$

Let $\delta_{ij} = \delta_i - \delta_j$. We use 0 and 1 as a shorthand notation for nodes 0^e and 1^e. We define the active and reactive power on the transmission line as

$$\begin{aligned}
P_{10} &= g_{10}|V_1|^2 - |V_0||V_1|(g_{10}\cos\delta_{10} + b_{10}\sin\delta_{10}) \\
P_{01} &= g_{01}|V_0|^2 - |V_0||V_1|(g_{01}\cos\delta_{01} - b_{01}\sin\delta_{01}) \\
Q_{10} &= -b_{10}|V_1|^2 - |V_0||V_1|(g_{10}\sin\delta_{10} - b_{10}\cos\delta_{10}) \\
Q_{01} &= -b_{01}|V_0|^2 + |V_0||V_1|(g_{01}\sin\delta_{01} + b_{01}\cos\delta_{01})
\end{aligned}$$

These are substituted into Equations (A3) and (A4). Hence, the active and reactive powers corresponding to the transmission line are no longer present in the system of equations. Instead the voltage magnitude and voltage angle are introduced into the system of equations.

For the heat network, assuming that $m_{0^h1^h} > 0$, the temperature at the end of a supply line and return line are substituted in the relevant equations by

$$\begin{aligned}
T^s_{1^h0^h} &= (T^s_{0^h1^h} - T^a)e^{\frac{-\lambda}{\overline{c_p}m_{0^h1^h}}L} + T^a \\
T^r_{0^h1^h} &= (T^r_{1^h0^h} - T^a)e^{\frac{-\lambda}{\overline{c_p}m_{0^h1^h}}L} + T^a
\end{aligned}$$

This leads to a system of 18 equations and 30 unknown variables whenever η_h is known.

Appendix C

Table A2. Physical properties of the electrical system.

	Variable	Value
	Power system	AC
Line	B (Susceptance)	-0.3 S
	G (Conductance)	0.03 S

Table A3. Physical properties of the gas system.

	Variable	Value
	Pressure system	Low pressure
	Gas type	Hydrogen gas
	HHV	$1.418 \cdot 10^8 \frac{\text{J}}{\text{kg}}$
	S (Specific gravity)	0.589
	Z (Compressibility factor)	1
	p_n (Standard pressure)	1 bar
	T_n (Standard temperature)	288 K
	R (Ideal gas constant)	$8.314413 \frac{\text{J}}{\text{molK}}$
	M (Molar mass of air)	$28.97 \cdot 10^{-3} \frac{\text{kg}}{\text{mol}}$
Pipe	L	500 m
	D	0.15 m
	f (Friction factor)	$6.5 \cdot 10^{-3}$

Table A4. Physical properties of the heat system.

	Variable	Value
	ρ (density of water)	$960 \frac{\text{kg}}{\text{m}^3}$
	C_p (Specific heat of water)	$4.182 \cdot 10^3 \frac{\text{J}}{\text{kgK}}$
	g (gravitational constant)	$9.81 \frac{\text{kg}}{\text{s}^2}$
	T_a (ambient temperature)	273.15 K
Pipe	L	500 m
	D	0.15 m
	λ (Heat transfer coefficient)	$0.2 \frac{\text{W}}{\text{m}^2\,\text{K}}$
	f (Friction factor)	$6.5 \cdot 10^{-3}$

Table A5. Electrolyzer efficiency.

Variable	Value
η	$\frac{9}{10}$
η_h	$\frac{1}{6}$

References

1. Lashof, D.A.; Ahuja, D.R. Relative contributions of greenhouse gas emissions to global warming. *Nature* **1990**, *344*, 529–531. [CrossRef]
2. Kweku, D.W.; Bismark, O.; Maxwell, A.; Desmond, K.A.; Danso, K.B.; Oti-Mensah, E.A.; Quachie, A.T.; Adormaa, B.B. Greenhouse Effect: Greenhouse Gases and Their Impact on Global Warming. *J. Sci. Res. Rep.* **2018**, *17*, 9. [CrossRef]
3. Amponsah, N.Y.; Troldborg, M.; Kington, B.; Aalders, I.; Hough, R.L. Greenhouse gas emissions from renewable energy sources: A review of lifecycle considerations. *Renew. Sustain. Energy Rev.* **2014**, *39*, 461–475. [CrossRef]
4. Kabeyi, M.J.B.; Olanrewaju, O.A. Sustainable Energy Transition for Renewable and Low Carbon Grid Electricity Generation and Supply. *Front. Energy Res.* **2022**, *9*, 743114. [CrossRef]
5. Kiaee, M.; Cruden, A.; Infield, D.; Chladek, P. Utilisation of alkaline electrolysers to improve power system frequency stability with a high penetration of wind power. *IET Renew. Power Gener.* **2014**, *8*, 529–536. [CrossRef]
6. Tuinema, B.W.; Adabi, E.; Ayivor, P.K.; García Suárez, V.; Liu, L.; Perilla, A.; Ahmad, Z.; Rueda Torres, J.L.; van der Meijden, M.A.; Palensky, P. Modelling of large-sized electrolysers for real-time simulation and study of the possibility of frequency support by electrolysers. *IET Gener. Transm. Distrib.* **2020**, *14*, 1985–1992. [CrossRef]
7. Samani, A.E.; D'Amicis, A.; De Kooning, J.D.; Bozalakov, D.; Silva, P.; Vandevelde, L. Grid balancing with a large-scale electrolyser providing primary reserve. *IET Renew. Power Gener.* **2020**, *14*, 3070–3078. [CrossRef]
8. van der Roest, E.; Bol, R.; Fens, T.; van Wijk, A. Utilisation of waste heat from PEM electrolysers – Unlocking local optimisation. *Int. J. Hydrog. Energy* **2023**, *48*, 27872–27891. [CrossRef]
9. Markensteijn, A.S.; Vuik, K.; Romate, J.E. On the Solvability of Steady-State Load Flow Problems for Multi-Carrier Energy Systems. In Proceedings of the 2019 IEEE Milan PowerTech, Milan, Italy, 23–27 June 2019; pp. 1–6. [CrossRef]
10. Markensteijn, A.; Romate, J.; Vuik, C. A graph-based model framework for steady-state load flow problems of general multi-carrier energy systems. *Appl. Energy* **2020**, *280*, 115286. [CrossRef]
11. Markensteijn, A.S.; Vuik, K. Convergence of Newton's Method for Steady-State Load Flow Problems in Multi-Carrier Energy Systems. In Proceedings of the 2020 IEEE PES Innovative Smart Grid Technologies Europe (ISGT-Europe), The Hague, The Netherlands, 26–28 October 2020; pp. 1084–1088. [CrossRef]
12. Zeng, Q.; Fang, J.; Li, J.; Chen, Z. Steady-state analysis of the integrated natural gas and electric power system with bi-directional energy conversion. *Appl. Energy* **2016**, *184*, 1483–1492. [CrossRef]
13. Zhang, L.; Ma, C.; Wang, L.; Wang, X. Theoretical analysis and economic evaluation of wind power consumption by electric boiler and heat storage tank for distributed heat supply system. *Electr. Power Syst. Res.* **2024**, *228*, 110060. [CrossRef]
14. Shi, Z.; Fan, F.; Tai, N.; Qing, C.; Meng, Y.; Guo, R. Coordinated Operation of the Multiple Types of Energy Storage Systems in the Green-Seaport Energy-Logistics Integrated System. *IEEE Trans. Ind. Appl.* **2024**, *60*, 4482–4493. [CrossRef]

15. De Corato, A.M.; Ghazavi Dozein, M.; Riaz, S.; Mancarella, P. Hydrogen Electrolyzer Load Modelling for Steady-State Power System Studies. *IEEE Trans. Power Deliv.* **2023**, *38*, 4312–4323. [CrossRef]
16. Zhang, N.; Yan, J.; Hu, C.; Sun, Q.; Yang, L.; Gao, D.W.; Guerrero, J.M.; Li, Y. Price-Matching-Based Regional Energy Market With Hierarchical Reinforcement Learning Algorithm. *IEEE Trans. Ind. Inform.* **2024**, *20*, 11103–11114. [CrossRef]
17. Schavemaker, P.; Sluis, L.v.d. *Electrical Power System Essentials*; John Wiley & Sons: Hoboken, NJ, USA, 2017.
18. Osiadacz, A.J.; Pienkosz, K. Methods of steady-state simulation for gas networks. *Int. J. Syst. Sci.* **1988**, *19*, 1311–1321. [CrossRef]
19. Savola, T.; Keppo, I. Off-design simulation and mathematical modeling of small-scale CHP plants at part loads. *Appl. Therm. Eng.* **2005**, *25*, 1219–1232. [CrossRef]
20. Werner, S. *District Heating and Cooling*; Elsevier: Amsterdam, The Netherlands, 2013. [CrossRef]
21. Clegg, S.; Mancarella, P. Integrated Modeling and Assessment of the Operational Impact of Power-to-Gas (P2G) on Electrical and Gas Transmission Networks. *IEEE Trans. Sustain. Energy* **2015**, *6*, 1234–1244. [CrossRef]
22. Jiang, Y.; Ren, Z.; Yang, X.; Li, Q.; Xu, Y. A steady-state energy flow analysis method for integrated natural gas and power systems based on topology decoupling. *Appl. Energy* **2022**, *306*, 118007. [CrossRef]
23. Zhao, P.; Gou, F.; Xu, W.; Shi, H.; Wang, J. Multi-objective optimization of a hybrid system based on combined heat and compressed air energy storage and electrical boiler for wind power penetration and heat-power decoupling purposes. *J. Energy Storage* **2023**, *58*, 106353. [CrossRef]
24. Demmel, J.W.; Gilbert, J.R.; Li, X.S. *SuperLU Users' Guide*; Technical Report LBNL–44289, 751785; National Energy Research Scientific Computing Center: Berkeley, CA, USA, 1999. [CrossRef]